Current-injection two-color lasing in a wafer-bonded coupled multilayer cavity with InGaAs multiple quantum wells

Yasuo Minami*, Hiroto Ota, Xiangmeng Lu, Naoto Kumagai†, Takahiro Kitada, and Toshiro Isu

Graduate School of Science and Technology, Tokushima University, Tokushima 770-8506, Japan

Current-injection two-color lasing has been demonstrated using a GaAs/AlGaAs coupled multilayer cavity that is a good candidate for novel terahertz-emitting devices based on difference-frequency generation (DFG) inside the structure. The coupled cavity structure was fabricated by the direct wafer bonding of (001)- and (113)B-oriented epitaxial wafers for the efficient DFG of two modes in the (113)B side cavity, and two types of InGaAs multiple quantum wells (MQWs) were introduced only in the (001) side cavity as optical gain materials. The threshold behavior was clearly observed in the current-light output curve even at room temperature. Two-color lasing was successfully observed when the gain peaks of MQWs were considerably tuned to the cavity modes by the operating temperature.

1. Introduction

Useful terahertz light sources have been extensively investigated because of the wide range of possible applications including wireless communication, spectroscopy, and imaging.[1,2] Recent femtosecond-laser technologies have made it possible to generate ultrashort terahertz pulses covering an extremely broad bandwidth range.[3–5] Several types of semiconductor-based devices such as quantum cascade lasers (QCLs),[6–8] resonant tunneling diodes (RTDs),[9,10] and photomixers[11,12] have also been studied and developed for continuous-wave terahertz emitters. Terahertz sources based on intracavity difference-frequency generation (DFG) in dual-wavelength midinfrared QCLs have also been recently reported.[13,14] However, there are still challenges associated with each of these devices. For example, the emission power becomes insufficient for the higher frequency operation of RTDs. In addition, although significant progress has been made on terahertz QCLs, near-room-temperature operation has not been demonstrated.

Optical microcavities are good candidates for nonlinear optical devices because an ex-

*E-mail: minami@tokushima-u.ac.jp
†Present address: National Institute of Advanced Industrial Science and Technology (AIST), Tsukuba 305-8560, Japan

tremely strong electric field is realized in a cavity layer sandwiched between two distributed Bragg reflector (DBR) multilayers. Efficient wavelength conversion is possible in a GaAs-based multilayer cavity when the structure is grown on a non-(001) substrate to allow the second-order nonlinearity of zincblende-type semiconductors.[15] In fact, blue vertical-cavity surface-emitting lasers (VCSELs) based on second-harmonic generation (SHG) on (113)B and (114)A GaAs substrates have been reported.[16] Recently, we have proposed a GaAs/AlAs coupled multilayer cavity structure for novel terahertz-emitting devices.[17] The structure consists of two equivalent cavity layers and three DBR multilayers, and it exhibits two cavity modes at the center of the high reflection band. This is because a degenerate cavity mode is split into two different modes as a result of the coupling of the cavity layers. Note that the mode frequency difference can be precisely defined within the terahertz region according to the number of intermediate DBR pairs. The electric field of each mode is greatly enhanced in both cavity layers, allowing strong frequency-mixed signals to be generated. Since the effective second-order nonlinear coefficient is zero on a (001)-oriented GaAs substrate owing to crystal symmetry,[15] a non-(001) substrate is essential for crystal growth. We have obtained a strong sum-frequency generation (SFG) signal from a GaAs/AlAs coupled multilayer cavity grown on a (113)B GaAs substrate when the two modes were simultaneously excited by 100 fs laser pulses.[18–20] The peak intensity of the SFG signal was more than 400 times greater than that of the SHG signal from the (113)B GaAs bulk substrate. DFG signals from the (113)B coupled cavity samples were also demonstrated at room temperature by time-resolved waveform measurements using 100 fs laser pulses and a photoconductive antenna.[21–23] In addition, we found that controlling the nonlinear polarization via the face-to-face bonding of two epitaxial wafers is an effective means of obtaining a large terahertz DFG signal from two modes.[24,25]

From the viewpoint of practical device applications, the two modes should be generated inside the structure by current injection, since this enables terahertz emission through DFG without external light sources. An ensemble of self-assembled InAs quantum dots (QDs) is a good candidate optical gain medium because the gain spectrum is broadened sufficiently such that it encompasses both cavity modes as a result of size inhomogeneity, whereas individual QDs have discrete electronic states. We have already demonstrated the two-mode emission by optical excitation using self-assembled InAs QDs that were inserted only in the upper cavity layer to realize optical gain in the near-infrared region.[26–28] Current-injection surface-emitting devices were also fabricated using a wafer-bonded coupled cavity in conjunction with QDs. However, the lasing behavior has not been observed yet because of the

insufficient optical gain of the QDs.[29] Note that Carlin and coworkers already demonstrated dual-wavelength lasing in two-section VCSELs by current injection at room temperature.[30,31] In the two-section VCSELs, both cavities had gain regions consisting of InGaAs multiple quantum wells (MQWs), and they also intentionally introduced asymmetry in the two-cavity length to stabilize dual-wavelength laser emissions. However, the use of two asymmetric cavities is unsuitable for the DFG of two modes through the second-order nonlinear response inside the structure because the field overlap between two modes is largely reduced by the weak coupling of two cavities. In our most recent study, we demonstrated two-color lasing from a strongly coupled two-cavity system that contains InGaAs MQWs with two different well widths solely in the upper cavity layer.[32] The coupled cavity structure of that study was formed without using the wafer bonding method and the two-color lasing of the current-injection device was observed under pulsed conditions at room temperature. In this study, we fablicated current-injection surface-emitting devices using a wafer-bonded coupled cavity containing InGaAs MQWs and investigated their emission properties.

2. Device fabrication

The coupled cavity structure must be fabricated by the face-to-face connection of two epi-wafers because the radiated terahertz fields from the two cavity layers largely cancel each other out owing to the phase mismatch when both cavity layers have the same second-order nonlinear susceptibility $\chi^{(2)}$.[24,25] Note that DFG through a second-order nonlinear process is forbidden on the (001) substrate owing to crystal symmetry, that is, $\chi^{(2)} = 0$, although pseudomorphic InGaAs MQWs with good optical properties are easily formed on the (001) GaAs substrate. On the other hand, the (113)B GaAs substrate gives a relatively large $\chi^{(2)}$ among high-index substrates while keeping good crystalline quality of the epitaxially grown GaAs/AlGaAs multilayer structure. In this study, two epiwafers were prepared by molecular beam epitaxy (MBE) on 3-inch-diameter (001)- and (113)B-oriented GaAs substrates.

Each epiwafer had a single cavity structure consisting of a GaAs-based 1.5-wavelength-thick ($3\lambda/2$) cavity and GaAs/$Al_{0.9}Ga_{0.1}As$ DBR multilayers. Two types of three-period $In_{0.15}Ga_{0.85}As$/GaAs MQWs, having a well width of either 3.6 or 4.4 nm, were embedded in the $3\lambda/2$ cavity of the (001) epiwafer, while a single GaAs layer without MQWs was used as the $3\lambda/2$ cavity of the (113)B epiwafer. Each MQW in the (001) side cavity was placed at the position where a strong electric field was realized for both modes. The thickness of each layer was set to a specific value so that the cavity modes would appear in the MQW emission peaks. Note that a slight lateral thickness variation was intentionally introduced only for the

(001) epiwafer to obtain a strongly coupled cavity system. Si and Be were used as the n-type and p-type dopants, respectively, to form a p-i-n junction of the current-injection-type device. To reduce the electrical series resistance, compositionally graded interfaces were used in each $GaAs/Al_{0.9}Ga_{0.1}As$ DBR multilayer. The doping concentration was approximately 2×10^{18} cm^{-3} for both the n- and p-type DBR multilayers, and a heavily Be-doped ($\sim 3 \times 10^{19}$ cm^{-3}) GaAs layer was used as the p-type contact layer. The two epiwafers were directly bonded at room temperature using the conventional surface-activated bonding method,[33,34] which is commonly used for the integration of two dissimilar semiconductor materials. Note that the structure of each epiwafer was designed to prevent optical loss at the bonding interface.[29] In the designed structure, the $\lambda/4$ GaAs layer nearest to the (113)B side cavity was replaced by a $3\lambda/4$ GaAs layer, and the bonding interface was set to a position being very close to the nodes in the electric field distributions of both modes. After the bonded wafer was cut into several chips with a size of 18×14 mm^2, the (001) GaAs substrate was completely removed by mechanical polishing and selective wet etching using a citric acid-based etchant[35] to form the current-injection devices. The number of pairs of the top, middle, and bottom DBRs of the coupled cavity structure were 28, 12.5, and 34, respectively.

Using the coupled cavity structure prepared as mentioned above, we fabricated the current-injection surface-emitting devices (Fig. 1) by the following procedure. First, circular mesas with diameters of 80–100 μm were formed via the following three-step wet etching process: (1) etching of the p-type DBR using a phosphoric acid solution, (2) selective etching of the upper cavity using a citric acid solution, and (3) selective etching of the topmost n-AlGaAs layer of the intermediate DBR using a more diluted phosphoric acid solution. To realize the current confinement structure, a 44.1-nm-thick AlAs layer inserted just above the upper cavity was selectively oxidized from the sidewall. The lateral oxidation of AlAs was accomplished by annealing at 480 °C under a steam environment, which was supplied by bubbling a nitrogen gas through deionized water maintained at 80 °C. Then, an n-type electrode was formed by depositing AuGe/Ni/Au (50 nm/12.5 nm/50 nm) onto the exposed n-type DBR surface, and mesas were buried in polyimide. Finally, p-type electrodes (Ti/Au) having optical windows were deposited on the p-type DBR surface, followed by rapid thermal annealing at 430 °C in nitrogen atmosphere.

3. Lasing characteristics

Optical emission characteristics of the devices were studied at room temperature using a pulsed-current source with a pulse duration of 1 μs and a duty cycle of 0.1%. The light emit-

ted from the optical window of each device was detected using an InGaAs p-i-n photodiode. The emission spectra at various injection currents were also measured using a spectrometer equipped with a cooled InGaAs photodiode array. Two sharp emission peaks due to the cavity modes were clearly observed in all the devices. Note that the frequency difference between two modes was systematically varied across the wafer because the (001) epiwafer was prepared to have a few percent thickness variation, whereas the lateral thickness of the (113)B epiwafer was as small as ~0.2%. Since two cavities with identical optical thicknesses were strongly coupled at the wafer position where the minimum frequency difference was observed, the devices located near this position were characterized in detail. The typical current-light output (*I*-*L*) curve is shown in Fig. 2. The threshold behavior was clearly observed in all the *I*-*L* curves measured at room temperature. Figure 3(a) shows the emission spectra measured at injection currents of 20 and 40 mA, which are below and above the threshold current (24 mA), respectively. Two peaks were observed in the spectrum below the threshold, while the lasing spectrum showed only a single peak corresponding to the long-wavelength mode. Figure 3(b) shows the photoluminescence (PL) spectrum of a reference MQW sample with the same layer structure as that used in the upper cavity of the device. Two broadened emission peaks of the InGaAs MQWs with two different well widths were observed on the longer-wavelength side compared with the cavity mode emissions. As can be seen in Fig. 3, the wavelength mismatch between the cavity modes and gain peaks of the MQWs caused the single-color lasing of the device.

The gain peaks can be tuned to the cavity modes by lowering the operating temperature because blue shifts of the MQW gain peaks are much larger than those of the cavity modes at lower temperatures. Using the same coupled cavity wafer as that used for room-temperature measurements, we fabricated different devices for low-temperature measurements, and a closed cycle cryostat was used to cool the devices. Figure 4 shows the intensities of the two mode emission peaks as functions of injection current for three different temperatures of 200, 190, and 180 K. The corresponding emission spectra acquired at 80 mA are also presented in this figure. At 200 K, the long-wavelength mode exhibited threshold behavior at a current of approximately 30 mA, which was not observed for the short-wavelength mode. Conversely, at 180 K, a threshold was only observed for the short-wavelength mode. In contrast to these two results, two-color lasing of both modes was successfully observed at the intermediate temperature of 190 K. The peak wavelengths were 904.4 and 911.6 nm, and the frequency difference was 2.6 THz. The results indicate that the intensity relationship in two-color lasing in the proposed device can be well tuned by the operating temperature.

Figure 5 shows the temperature dependence of the emission spectra at an injection current of 80 mA. Two-color lasing was observed in the temperature range of 192 to 180 K. Let us compare each spectrum of the device with the PL of the reference MQW sample, which is plotted by a dashed curve in Fig. 5. Surprisingly, the PL peaks disagreed with the cavity modes in the temperature range where two-color lasing was observed. In this temperature range, the PL peaks were observed at shorter wavelengths than the cavity modes. Thus, the actual temperature of the active region was considered to be elevated even for the pulsed operation of two-color lasing. From the PL spectra of the reference MQW sample in the temperature range of 160–220 K, the temperature rise of ~30 K was roughly estimated at the active region current when the two-color lasing of the device was induced by current injection. We can also explain the behavior observed in the current dependence of two-mode intensities by a temperature increase in the active region. As shown in Fig. 4, the short-wavelength mode initially oscillated with increasing current, and then the intensity saturated with further current increase. The long-wavelength mode oscillated at higher injection currents. These results are well explained by the fact that the red shifts of MQW peaks increase with increasing current. Since the temperature of the active region seemed to gradually elevate with increasing current, thermal dissipation should be carefully managed for actual device operation.

4. Conclusions

Current-injection two-color lasing has been demonstrated in a wafer-bonded GaAs/AlGaAs coupled multilayer cavity that contains InGaAs MQWs as optical gain materials. The structure was fabricated by the direct wafer bonding of the (001) and (113)B epitaxial wafers prepared individually by MBE. The InGaAs MQWs with two different well widths were introduced only in the (001) side cavity. The current-injection surface-emitting devices were fabricated using the wafer-bonded coupled cavity. Although the threshold behavior was clearly observed in the *I*-*L* curve at room temperature, the spectrum showed the single-color lasing of the device. Two-color lasing was successfully achieved when the gain peaks of MQWs were considerably tuned to the cavity modes by lowering the operating temperature. We also found that the lasing of two colors with identical intensities is induced by the fine tuning of the operating temperature or injection current, which is very useful for the proposed terahertz-emitting devices based on the DFG.

Acknowledgment

This work was partly supported by a Grant-in-Aid for Scientific Research (B) (No. 16H04351) from the Japan Society for the Promotion of Science (JSPS).

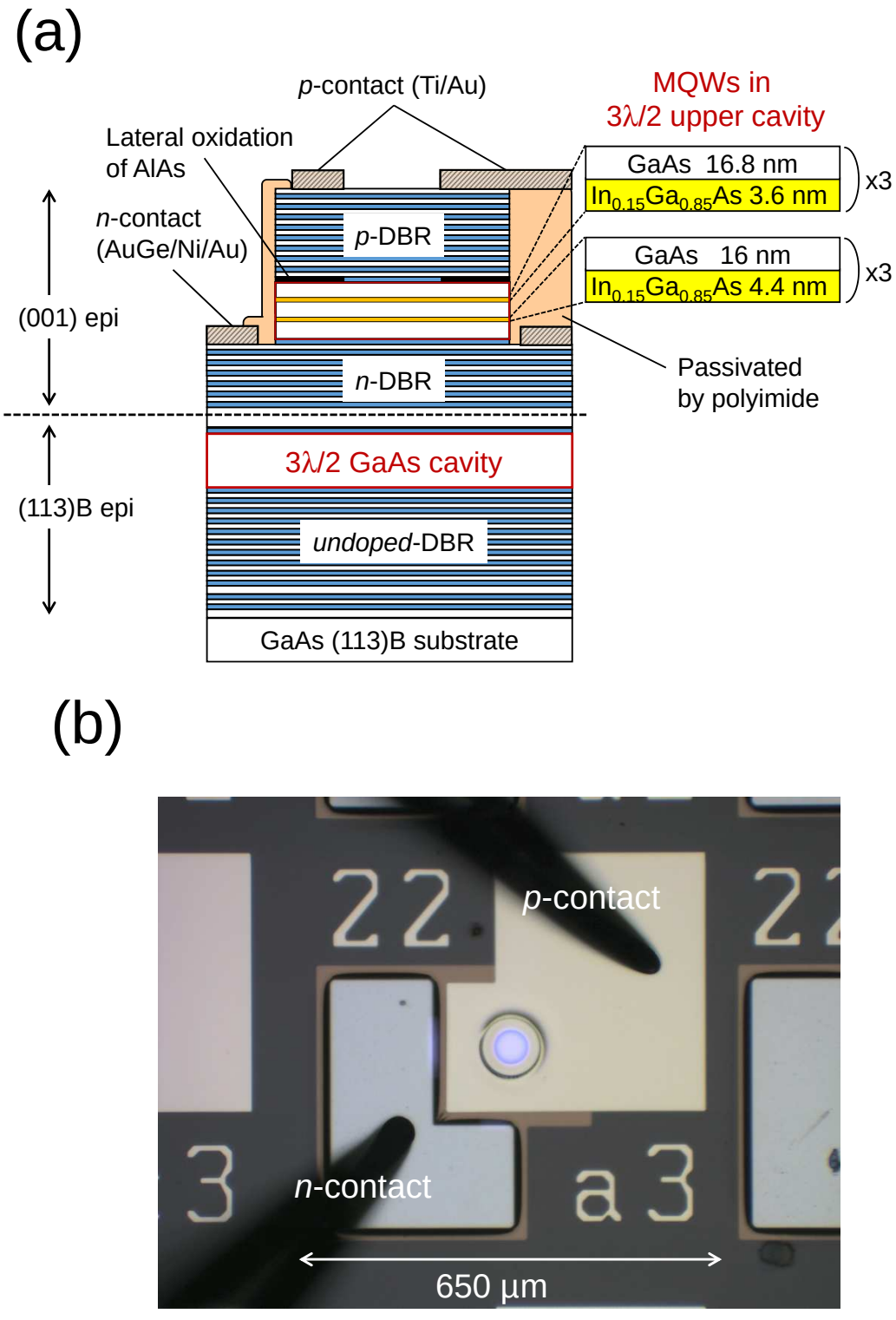

Fig. 1. (Color online) (a) Schematic of the current-injection device based on a GaAs/AlGaAs couple multilayer cavity fabricated by wafer bonding of two epitaxial wafers. (b) Top view of the fabricated device.

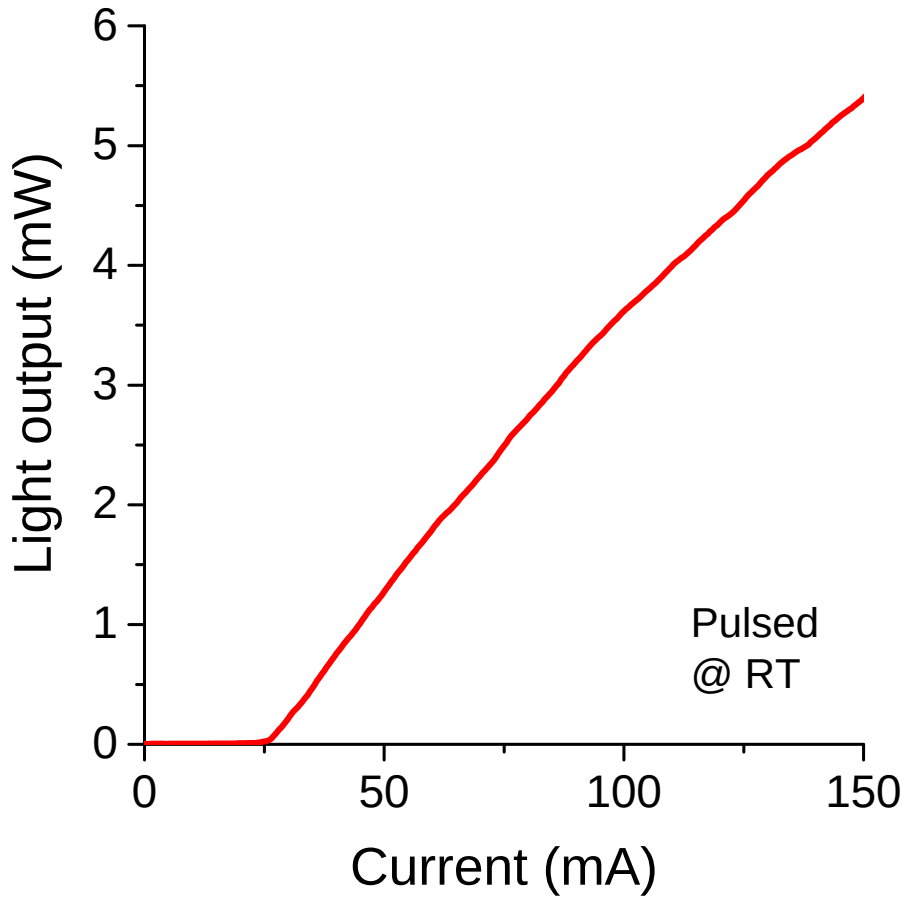

Fig. 2. (Color online) Current-light output curve measured under room-temperature pulsed operation.

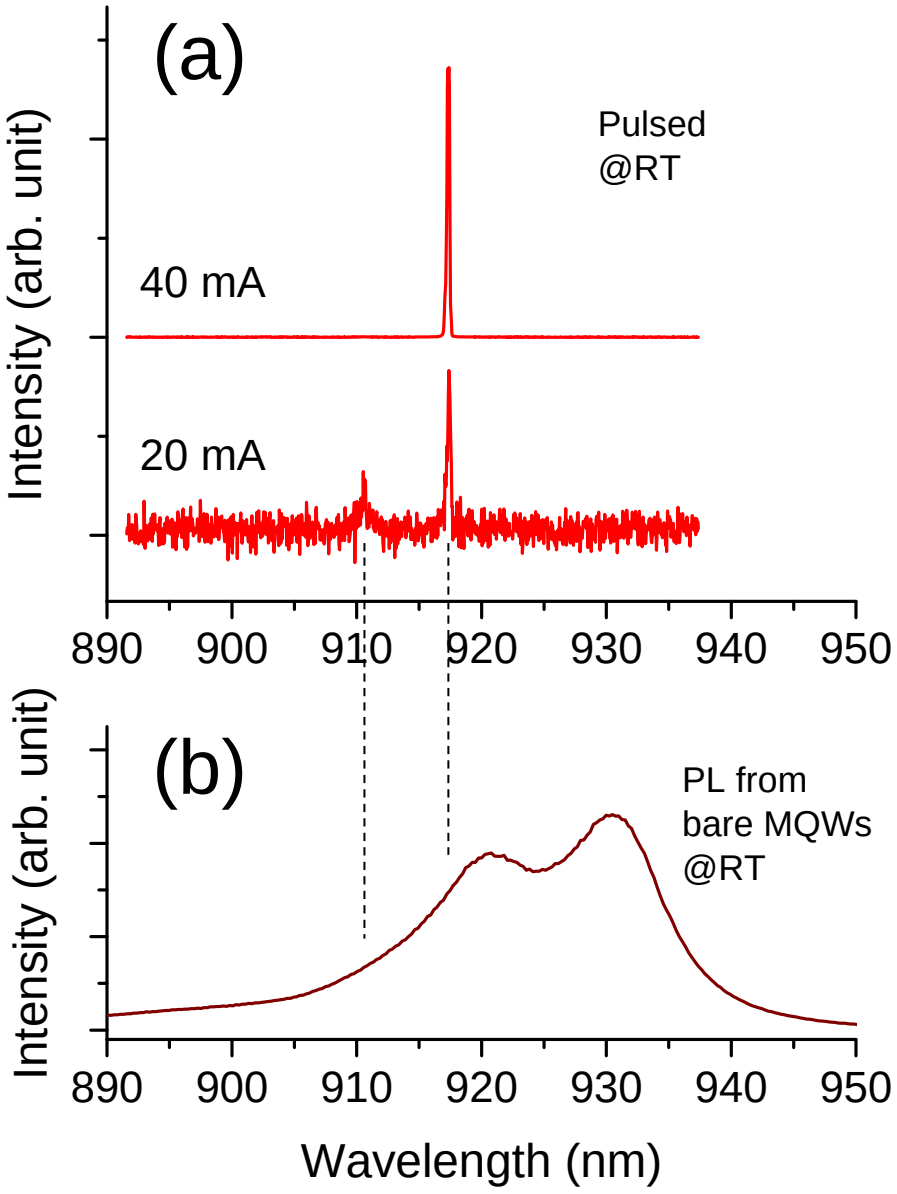

Fig. 3. (Color online) (a) Emission spectra of the device measured at injection currents of 20 and 40 mA, which are below and above the threshold current, respectively. (b) PL spectrum measured for a reference MQW sample with the same layer structure as that used in the upper cavity.

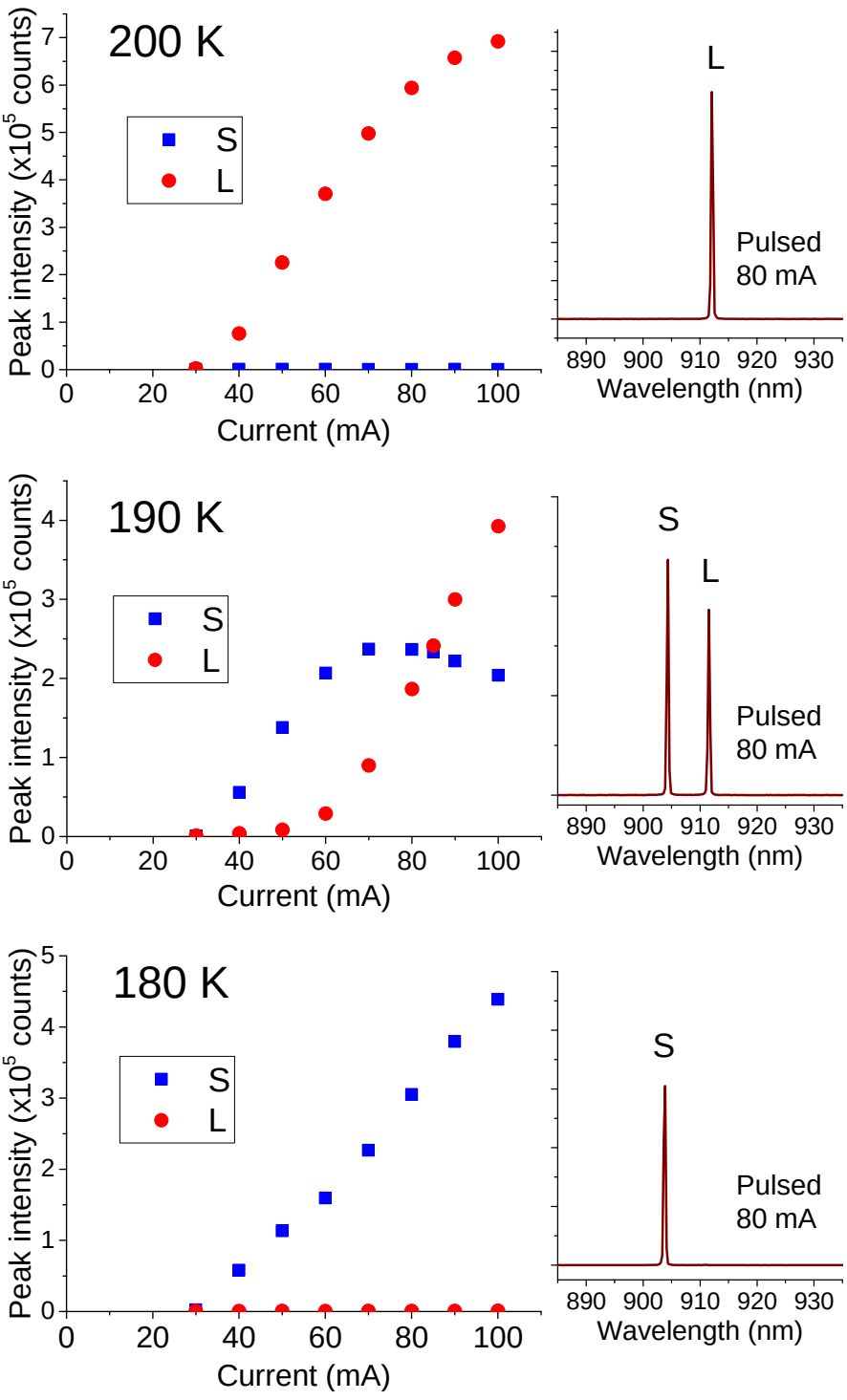

Fig. 4. (Color online) Peak emission intensities of the two modes plotted as functions of injection current measured at three different temperatures of 200, 190, and 180 K. Each right-hand panel shows the corresponding lasing spectrum measured at an injection current of 80 mA.

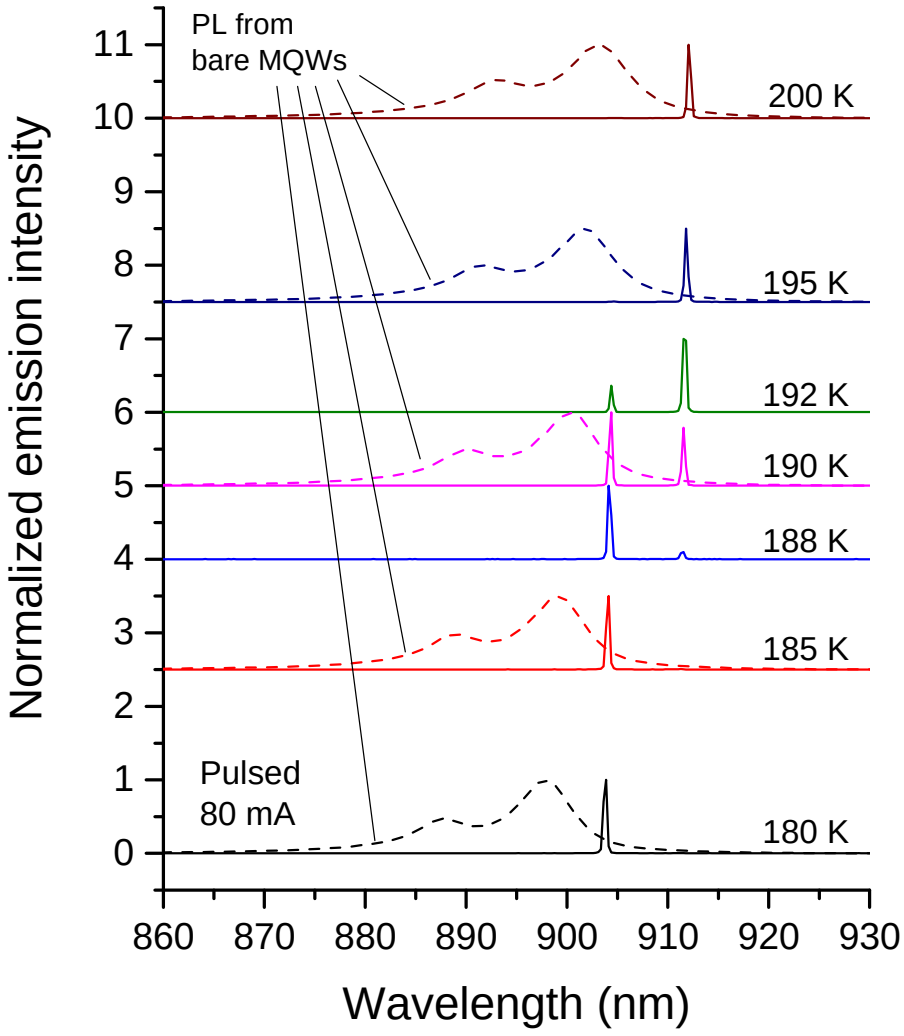

Fig. 5. (Color online) Temperature dependence of the emission spectrum at an injection current of 80 mA. Each broken line indicates the PL spectrum of a reference MQW sample measured at the corresponding temperature.

References

1) M. Tonouchi, Nat. Photonics **1**, 97 (2007).
2) W. L. Chan, J. Deibel, and D. M. Mittleman, Rep. Prog. Phys. **70**, 1325 (2007).
3) D. H. Auston, K. P. Cheung, and P. R. Smith, Appl. Phys. Lett. **45**, 284 (1984).
4) P. Y. Han and X.-C. Zhang, Appl. Phys. Lett. **73**, 3049 (1998).
5) M. Nagai, K. Tanaka, H. Ohtake, T. Bessho, T. Sugiura, T. Hirosumi, and M. Yoshida, Appl. Phys. Lett. **85**, 3974 (2004).
6) R. Köhler, A. Tredicucci, F. Beltram, H. E. Beere, E. H. Linfield, A. G. Davies, D. A. Ritchie, R. C. Iotti, and F. Rossi, Nature **417**, 156 (2002).
7) B. S. Williams, Nat. Photonics **1**, 517 (2007).
8) M. A. Belkin, J. A. Fan, S. Hormoz, F. Capasso, S. P. Khanna, M. Lachab, A. G. Davies, and E. H. Linfield, Opt. Express **16**, 3242 (2008).
9) M. Asada, S. Suzuki, and N. Kishimoto, Jpn. J. Appl. Phys. **47**, 4375, (2008).
10) S. Suzuki, M. Asada, A. Teranishi, H. Sugiyama, and H. Yokoyama, Appl. Phys. Lett. **97**, 242102 (2010).
11) S. Matsuura, M. Tani, and K. Sakai, Appl. Phys. Lett. **70**, 559 (1997).
12) H. Ito, F. Nakajima, T. Furuta, K. Yoshino, and T. Ishibashi, Electron. Lett. **39**, 1828 (2003).
13) K. Vijayraghavan, Y. Jiang, M. Jang, A. Jiang, K. Choutagunta, A. Vizbaras, F. Demmerle, G. Boehm, M. C. Amann, and M. A. Belkin, Nat. Commun. **4**, 2021 (2013).
14) K. Fujita, M. Hitaka, A. Ito, T. Edamura, M. Yamanishi, S. Jung, and M. A. Belkin, Appl. Phys. Lett. **106**, 251104 (2015).
15) N. Yamada, Y. Ichimura, S. Nakagawa, Y. Kaneko, T. Takeuchi, and N. Mikoshiba, Jpn. J. Appl. Phys. **35**, 2659 (1996).
16) Y. Kaneko, S. Nakagawa, Y. Ichimura, and N. Yamda, J. Appl. Phys. **87**, 1597 (2000).
17) T. Kitada, F. Tanaka, T. Takahashi, K. Morita, and T. Isu, Appl. Phys. Lett. **95**, 111106 (2009).
18) F. Tanaka, T. Takahashi, K. Morita, T. Kitada, and T. Isu, Jpn. J. Appl. Phys. **49**, 04DG01 (2010).
19) K. Morita, F. Tanaka, T. Takahashi, T. Kitada, and T. Isu, Appl. Phys. Express **3**, 072801 (2010).
20) F. Tanaka, T. Takimoto, K. Morita, T. Kitada, and T. Isu, Jpn. J. Appl. Phys. **50**, 04DG03 (2011).

21) K. Morita, S. Katoh, T. Takimoto, F. Tanaka, Y. Nakagawa, S. Saito, T. Kitada, and T. Isu, Appl. Phys. Express **4**, 102102 (2011).
22) S. Katoh, T. Takimoto, Y. Nakagawa, K. Morita, T. Kitada, and T. Isu, Jpn. J. Appl. Phys. **51**, 04DG05 (2012).
23) T. Kitada, S. Katoh, T. Takimoto, Y. Nakagawa, K. Morita, and T. Isu, IEEE Photonics J. **5**, 6500308 (2013).
24) T. Kitada, F. Tanaka, T. Takahashi, K. Morita, and T. Isu, Proc. SPIE **7937**, 79371H (2011).
25) T. Kitada, S. Katoh, T. Takimoto, Y. Nakagawa, K. Morita, and T. Isu, Appl. Phys. Lett. **102**, 251118 (2013).
26) T. Kitada, C. Harayama, K. Morita, and T. Isu, Phys. Status Solidi C **10**, 1434 (2013).
27) C. Harayama, S. Katoh, Y. Nakagawa, K. Morita, T. Kitada, and T. Isu, Jpn. J. Appl. Phys. **53**, 04EG11 (2014).
28) C. Harayama, S. Katoh, Y. Nakagawa, X. M. Lu, N. Kumagai, T. Kitada, and T. Isu, Jpn. J. Appl. Phys. **54**, 04DG10 (2015).
29) H. Ota, X. M. Lu, N. Kumagai, T. Kitada, and T. Isu, Jpn. J. Appl. Phys. **55**, 04EH09 (2016).
30) J. F. Carlin, R. P. Stanley, P. Pellandini, U. Oesterle, and M. Ilegems, Appl. Phys. Lett. **75**, 908 (1999).
31) M. Brunner, K. Gulden, R. Hövel, M. Moser, J. F. Carlin, R. P. Stanley, and M. Ilegems, IEEE Photonics Technol. Lett. **12**, 1316 (2000).
32) T. Kitada, H. Ota, X. M. Lu, N. Kumagai, and T. Isu, Appl. Phys. Express **9**, 111201 (2016).
33) T. R. Chung, L. Yang, N. Hosoda, H. Takagi, and T. Suga, Appl. Surf. Sci. **117-118**, 808 (1997).
34) H. Takagi, K. Kikuchi, R. Maeda, T. R. Chung, and T. Suga, Appl. Phys. Lett. **68**, 2222 (1996).
35) T. Kanbara, S. Nakano, S. Yano, K. Morita, T. Kitada, and T. Isu, Jpn. J. Appl. Phys. **48**, 04C105 (2009).